Testing the $^{231}Pa/^{230}Th$ paleocirculation proxy: A data versus 2D model comparison

Jörg Lippold,[1] Jeanne-Marie Gherardi,[2,3] and Yiming Luo[4]

Received 12 August 2011; revised 26 September 2011; accepted 28 September 2011; published 29 October 2011.

[1] Variations of the Atlantic Meridional Overturning Circulation (AMOC) are believed to have crucially influenced Earth's climate due to its key role in the inter-hemispheric redistribution of heat and carbon. To assess its past strength, the sedimentary $^{231}Pa/^{230}Th$ proxy has been developed and improved but also contested due to its sensitivity to other factors beyond ocean circulation. In order to provide a better basis for the understanding of the Atlantic $^{231}Pa/^{230}Th$ system, and therefore to shed light on the controversy, we compare new measurements of Holocene sediments from the north Brazilian margin to water column data and the output of a two-dimensional scavenging-circulation model, based on modern circulation patterns and reversible scavenging parameters. We show that sedimentary $^{231}Pa/^{230}Th$ data from one specific area of the Atlantic are in very good agreement with model results suggesting that sedimentary $^{231}Pa/^{230}Th$ is predominantly driven by the AMOC. Therefore, $^{231}Pa/^{230}Th$ represents an appropriate method to reconstruct past AMOC at least qualitatively along the western margin. **Citation:** Lippold, J., J.-M. Gherardi, and Y. Luo (2011), Testing the $^{231}Pa/^{230}Th$ paleocirculation proxy: A data versus 2D model comparison, *Geophys. Res. Lett.*, *38*, L20603, doi:10.1029/2011GL049282.

1. Introduction

[2] The sedimentary $^{231}Pa_{xs,0}/^{230}Th_{xs,0}$ reflects the activity ratios of ^{231}Pa and ^{230}Th produced by decay of uranium in the water column and scavenged to the sea floor. (Pa/Th hereafter). Because U isotopes are evenly distributed in the ocean, the production rate of ^{231}Pa and ^{230}Th is constant in the oceanic water column. The usage of sedimentary Pa/Th to reconstruct past changes in the rate and geometry of the Atlantic Meridional Overturning Circulation (AMOC) [*McManus et al.*, 2004; *Yu et al.*, 1996], relies on the fact that ^{231}Pa has a longer residence time in the water column than ^{230}Th [*Anderson et al.*, 1983; *Nozaki and Nakanishi*, 1985]. The residence time of ^{230}Th is short enough to limit severely the extent to which it can be laterally transported after it is produced by the radioactive decay of uranium. By contrast, as a result of its longer residence time, ^{231}Pa is widely distributed via the ocean's circulation.

[3] Thus, low Pa/Th in North Atlantic sediments has been interpreted as an indicator for an active AMOC at the time of deposition, while Pa/Th in the range of the production ratio (activity ratio = 0.093) would be expected in times of low or even zero circulation strength [*Marchal et al.*, 2000; *McManus et al.*, 2004].

[4] However, such an approach has been contested based on the temporal variability of the fractionation between ^{231}Pa and ^{230}Th due to changes in particle fluxes and composition [*Bradtmiller et al.*, 2007; *Keigwin and Boyle*, 2008; *Lippold et al.*, 2009], inconsistency with water column data [*Anderson et al.*, 2009], or because of the spatial coverage of the data set [*Gherardi et al.*, 2010; *Peacock*, 2010]. Thus, in order to improve understanding of the Pa/Th system we compare data from a defined area of the Atlantic Ocean along the flow path of the western boundary current, temporally constrained to the late Holocene, to model predictions.

[5] New measurement results and records from the area available from literature (sediment and water column data) were compared to results of a 2D box model [*Luo et al.*, 2010] to test the role of the strength of AMOC in dominating the sedimentary Pa/Th signal.

2. Study Area

[6] We focus our study on a depth transect from the north Brazilian margin sector of the Atlantic Ocean. Water column records of hydrological properties indicate that this sector is bathed by the main components of the AMOC (Figures 1a and 1b) and Figure 2 of *Schott et al.* [2003]. The warm surface waters flowing northward from the Brazilian current are overlie the Antarctic Intermediate Water (AAIW) covering a depth range from 500 to 900 meters. Below this, from 900 to 1500 meters, the Circumpolar Deep Water Current (CPDW) is flowing northward. The North Atlantic Deep Water (NADW) flows southward between 1500 and 3800 m, constituting the main component of deep water in this sector. The bottom water is characterised by a northward flow of cold Antarctic Bottom Water (AABW) [*Schott et al.*, 2003]. This sector is ideal to capture the main features of the AMOC and therefore to identify the influence of water mass export on sedimentary Pa/Th redistribution.

[7] We focus on late Holocene sediments only (<2.8 ka, see Table S1 in the auxiliary material).[1] Although there might have been variations of the AMOC during this time period [*Keigwin and Boyle*, 2000], these variations are expected to be minor from a glacial/interglacial perspective and too weak with respect to the sensitivity (and partly time resolution) of the Pa/Th proxy. Thus, for this study we presume a steady-state AMOC for the late Holocene within the last 3 ka. In support of this assumption, North Atlantic Pa/Th time series profiles [*Bradtmiller et al.*, 2007; *Gherardi et al.*, 2009; *Hall*

[1]Heidelberg Academy of Sciences, Institute of Environmental Physics, University of Heidelberg, Heidelberg, Germany.
[2]LSCE, IPSL, CNRS/CEA/UVSQ, Gif-sur-Yvette, France.
[3]Bjerknes Center for Climate Research, Institut for Geovitenskap, University of Bergen, Bergen, Norway.
[4]Department of Earth and Ocean Sciences, University of British Columbia, Vancouver, British Columbia, Canada.

0094-8276/11/2011GL049282

[1]Auxiliary materials are available in the HTML. doi:10.1029/2011GL049282.

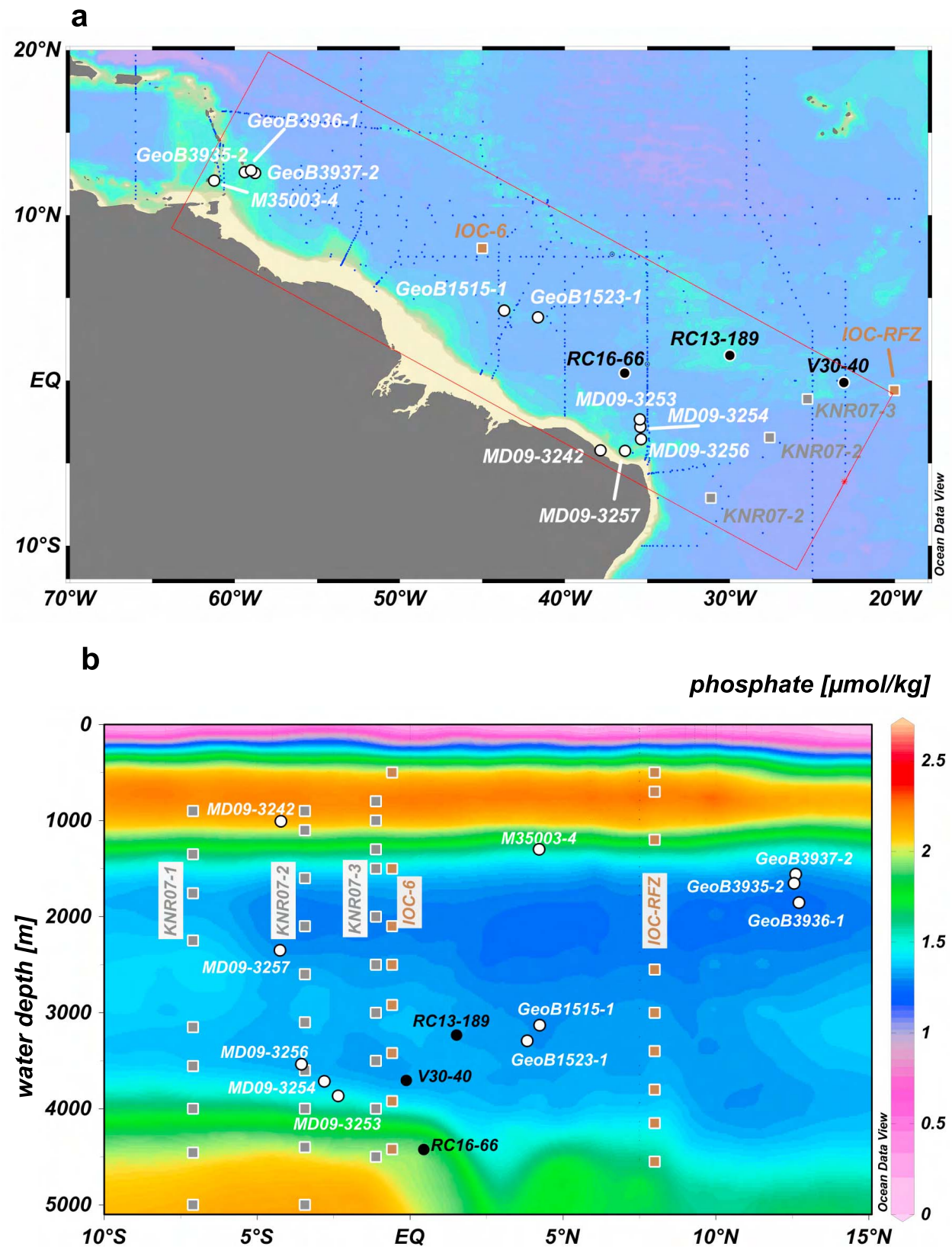

Figure 1. (a) Region of study: sediment samples are marked with white (this study) and black [*Bradtmiller et al.*, 2007]; water column data is indicated in grey [*Luo et al.*, 2010] and brown [*Moran et al.*, 2002]. The red box marks the section from which data has been extracted to display water masses in Figure 1b. (b) Water depth of sedimentary Pa/Th samples (white (this study), black [*Bradtmiller et al.*, 2007]) and water station locations (grey [*Luo et al.*, 2010], brown [*Moran et al.*, 2002]) along a CARINA bottle data section of total phosphate in the water (μmol/kg) as water masses indicator from 12°S to 15°N [*Tanhua et al.*, 2009].

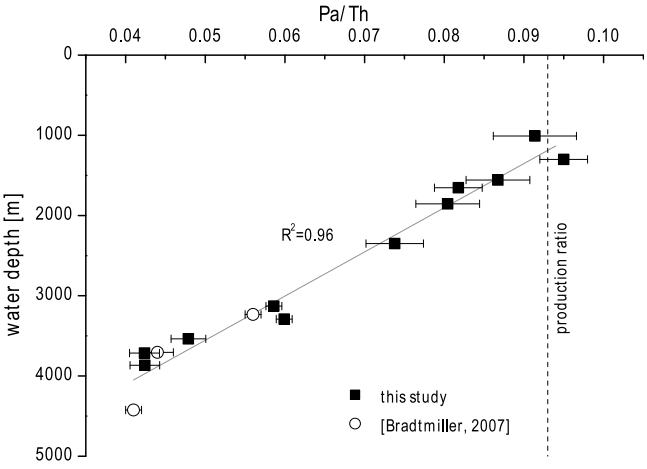

Figure 2. Sedimentary Pa/Th (in black, this study) and *Bradtmiller et al.*'s [2007] data (white). Production ratio of 0.093 is represented by the dashed line. The good linear correlation with a correlation coefficient of 0.96 is shown by the black regression line.

et al., 2006; *McManus et al.*, 2004] have not recorded any significant variations in their most recent record sections.

[8] We extended available sedimentary Pa/Th data from this area [*Bradtmiller et al.*, 2007] by measuring recently recovered core tops from cruise (MD 173/RETRO-3, (Calypso Square cores MD09-3242CQ, MD09-3253CQ, MD09-3254CQ, MD09-3256CQ, and calypso piston core MD09-3257) and late Holocene samples from GeoB3935-2, GeoB3936-1, GeoB3937-2, GeoB1515-1, GeoB1523-1, and M35003-4 spanning the depth range of 1000 to 4000 m along the western boundary current [*Dengler et al.*, 2004]. All cores are located along the north Brazilian margin between 13°N to 4°S within the pathway of the western boundary current (details are listed in Table S1). Sedimentary Pa/Th is compared to dissolved and particulate ^{231}Pa and ^{230}Th concentrations derived from published water column measurements [*Luo et al.*, 2010; *Moran et al.*, 2002] made within the studied area.

3. Results

3.1. Sedimentary Pa/Th

[9] Measurements were made by ICP-MS enabling high accuracy and high reproducibility. Two samples have been measured twice to proof reproducibility (better than 2.5% for complete Pa/Th replicates) of the applied method (for further details regarding measurement methods, please see Text S1).

[10] The sedimentary Pa/Th depth profile reveals a remarkably close correlation with water depth in this area under the influence of the western boundary current (Figure 2). The deeper part of the water column below 3000 m is represented by 8 sedimentary Pa/Th data and shows values significantly below the production ratio (Pa/Th from 0.042 to 0.062 between 3000 and 4500 m). Shallower cores above 2000 m show significantly higher Pa/Th reaching the production ratio level at about 1300 m (5 sedimentary Pa/Th values ranging from 0.08 to 0.094 between 2000 and 1000 m). One sedimentary Pa/Th data point between 2000 and 3000 m fits well within a linear trend between the shallow and deep sites (Pa/Th = 0.074). The overall trend closely follows a linear correlation (Figure 2, $R^2 > 0.9$). We do not observe significant disparities between data of *Bradtmiller et al.* [2007] and our new data set.

3.2. Fractionation Factor

[11] The differential removal of ^{230}Th and ^{231}Pa from the open ocean or the degree to which particle composition may affect the fractionation of ^{231}Pa and ^{230}Th can be expressed in terms of a fractionation factor [*Anderson et al.*, 1983].

$$F = (Pa/Th)_{diss}/(Pa/Th)_{part}$$

where $(Pa/Th)_{diss}$ is the ratio of dissolved ^{231}Pa and ^{230}Th concentrations, and $(Pa/Th)_{part}$ is the ratio of the suspended particulate ^{231}Pa and ^{230}Th concentrations.

[12] Within our area of examination, two depth profiles (IOC-6 and IOC-RFZ) [*Moran et al.*, 2002] of dissolved (Figure 3a, open circles) and particulate Pa/Th and thus F is available (Figure 3b, open circles). Additionally, water column data of dissolved Pa/Th is available from three depth profiles (KNR07−1,−2 and −3 [*Luo et al.*, 2010]). To further examine a potential influence of F on the depth correlation of Pa/Th we calculated F using the new sedimentary Pa/Th ratios instead of those on suspended particles. To do so an interpolation of the combined water column data of *Moran et al.* [2002] and *Luo et al.* [2010] (Figure 3a, open circles) from this region was generated in order to associate each sedimentary Pa/Th ratio of our data set (Figure 3a, black squares) to an interpolated dissolved Pa/Th ratio at the same depth. This leads us to an alternative estimation of F, even though it implies larger error bars due to the deviation from the measurement values to the depth interpolation. For our data, F varies between 7.7 to 10.3 within the same range of variation than when F is calculated using dissolved and particulate ratios from water column stations IOC-RFZ and IOC-6 (from 6.3 to 12.0) [*Moran et al.*, 2001, 2002]. Thus, both data sets show large variations in F, but no particular depth dependency can be observed for our studied area.

[13] It has been suggested that ^{231}Pa and ^{230}Th are scavenged to the sea floor from within approximately 1000 m of the sea floor [*Thomas et al.*, 2006]. When calculating F from dissolved water column Pa/Th and sedimentary Pa/Th instead of particulate Pa/Th, this may cause a systematic bias to lower F when the water is at the same depth as the sediment being used (because Pa/Th of the water column changes with depth). To test the significance of this bias we calculate F by assuming a shift of 500 m (middle of the relevant water column box above the bottom) of the interpolated dissolved fraction compared to the sedimentary data (Figure 3b, grey). This way obtained values are systematically shifted toward higher F, and show a better agreement to the F calculated by *Moran et al.* [2002] for the upper 2500 m. Below, the values seem to overestimate the fractionation compared to *Moran et al.* [2002]. This implies that in shallower water the Pa/Th signature of surrounding waters is carried down with particles from more than 1000 m above, while in deeper waters this range seems to be lower. However, these findings should be examined and discussed in light of new water column measurements and do not affect our main finding that F

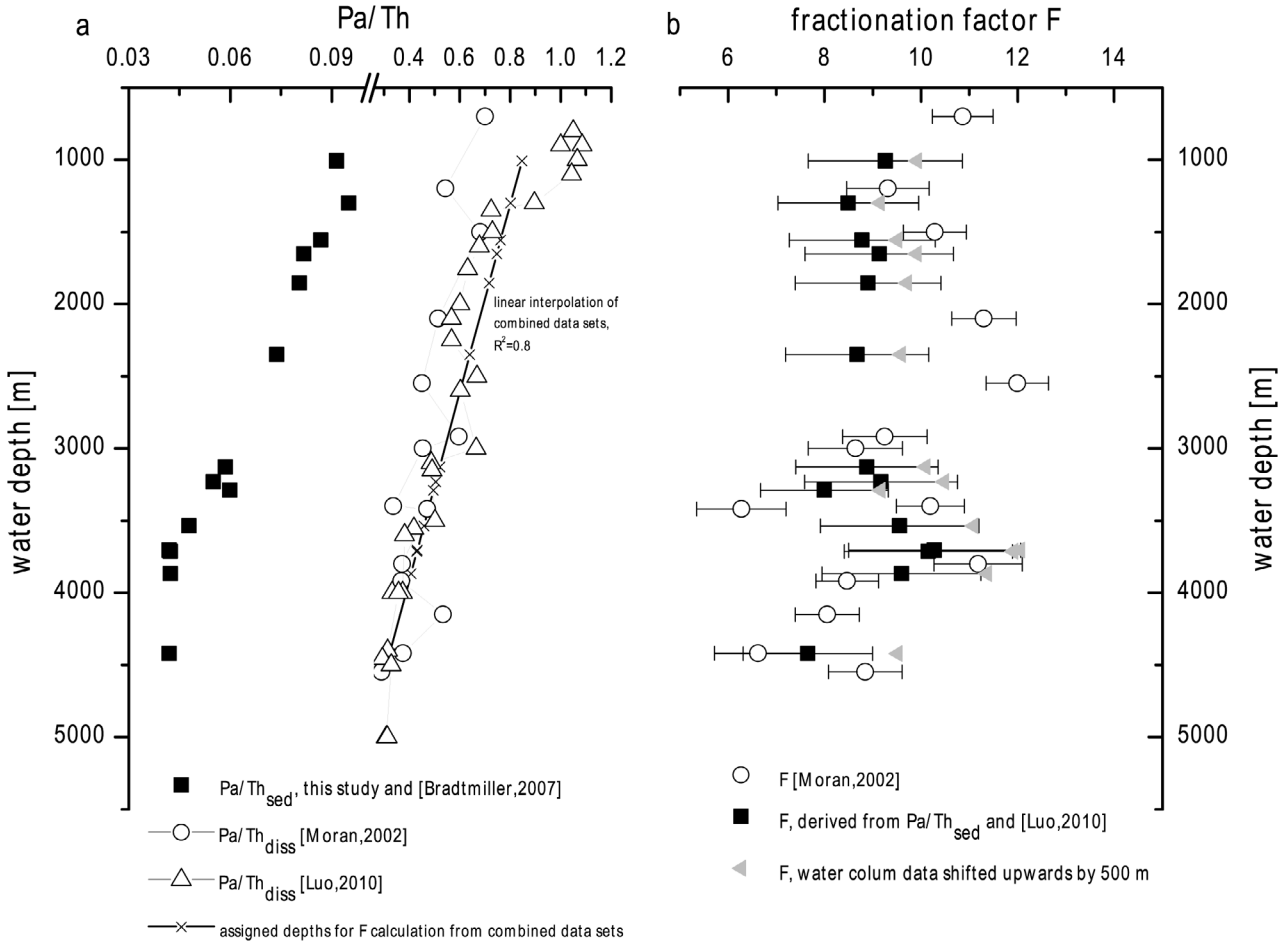

Figure 3. (a) Sedimentary Pa/Th (black) from this study and combined dissolved Pa/Th data from *Moran et al.* [2001, 2002] (open circles) and *Luo et al.* [2010] (open triangles) plotted versus depth. Note that the x-scale is different between sedimentary and dissolved data. (b) Fractionation factor F plotted versus depth. Although F is estimated using a different approach in this study compared to *Moran et al.* [2002], very similar results are obtained. Open circles: F-factor from two sites combined from [*Moran et al.*, 2001, 2002]; black squares: F-Factor from sedimentary Pa/Th (this study) and water column data [*Luo et al.*, 2010]; grey triangles: F-factor from sedimentary Pa/Th (this study) and water column data [*Luo et al.*, 2010], but by assuming a shift of 500 m from the interpolated dissolved fraction compared to the sedimentary (see text).

obviously does not systematically change with water depth in this region.

4. Discussion

4.1. Fractionation or Circulation?

[14] Sedimentary Pa/Th is a function of both the availability of ^{231}Pa and ^{230}Th in the water column (i.e., the dissolved Pa/Th ratio) and their fractionation while being scavenged by particles from the water column. The fractionation is determined by the total flux of particles and the composition of the particle flux while variable dissolved ratios can be related to differences in scavenging intensities or differences in isotope composition of water masses. Thus, when sedimentary Pa/Th shows depth-dependent variations, at least one of these parameters is expected to be responsible for the course of the Pa/Th profiles.

[15] The Pa/Th close to or higher than the production rate of 0.093 are often associated with preferential scavenging of ^{231}Pa compared to ^{230}Th caused by high opal abundance. However, if this was the case, this should be reflected in lower F-factors. In our context, we do not observe such a decrease of the F-factor in shallower waters. In addition, in the late Holocene the western equatorial Atlantic is characterized by low productivity resulting in minima in biogenic opal fluxes [*Bradtmiller et al.*, 2007]. Preserved fluxes of biogenic opal available for GeoB1515-1, Geob1523-1, GeoB3935-2, GeoB3937-2, GeoB3936-1 (this study) and RC13-189, RC16-66 and V30-40 [*Bradtmiller et al.*, 2007] do not exceed 0.05 g/cm^2/ka (see Table S1) and are therefore in strong agreement with the low productivity context. Thus, it is very unlikely that local impacts of biogenic opal may bias the shallowest core-top's sedimentary Pa/Th signal concerned in this study. More generally, the fact that the F-factor is not correlated to water depth over the entire water column (Figure 3b) suggests that changes in the particle composition (e.g., caused by preferential dissolution of biogenic opal in deep waters [*Scholten et al.*, 2008]) are not responsible for the decrease of sedimentary Pa/Th with depth.

[16] The dissolved Pa/Th signal that reflects NADW export in the water column can be transferred to the sedimentary Pa/Th provided that the fractionation between ^{231}Pa and

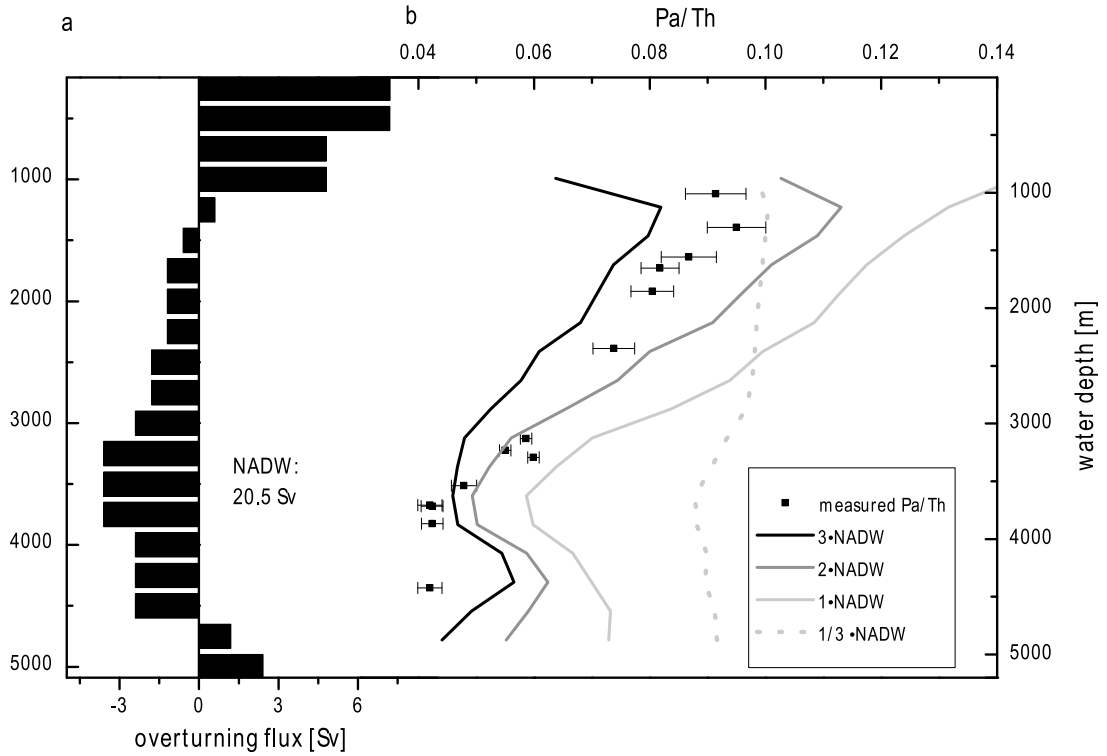

Figure 4. (a) Lateral water transport in the Atlantic Ocean at the Equator as assumed as model input. The NADW strength assumed here is 20.5 Sv [*Luo et al.*, 2010]. To adapt the basin-wide model to the specific situation (narrower basin) at the northern Brazilian margin, NADW strength can be modified (and herewith the northward compensatory surface currents. (b) Model output at the latitude 1.25° N for varying NADW strength (factors of 1/3, 1, 2 and 3 of 20.5 Sv) compared to measured sedimentary Pa/Th (black squares).

^{230}Th in the water column is not depth-dependent, as just demonstrated. Thus, we conclude that the new sedimentary Pa/Th presented here mirrors the contribution of the dissolved phase, which is a function of AMOC.

[17] Such a distribution of high Pa/Th in shallower waters and low Pa/Th in deep water is predicted for a vigorous export of ^{231}Pa with an advection of deep waters to the Southern Ocean [*Francois*, 2007; *Gherardi et al.*, 2010; *Luo et al.*, 2010].

[18] In absence of lateral transport by currents, particulate transport balances the in situ production. In this case, the vertical profiles of both ^{230}Th and ^{231}Pa are expected to increase linearly with depth, as predicted by reversible scavenging models [*Bacon and Anderson*, 1982; *Roy-Barman*, 2009]. Deviations from a linear profile indicate that oceanic currents carry significant amounts of ^{230}Th and ^{231}Pa away from their production site [*Coppola et al.*, 2006; *Marchal et al.*, 2000; *Roy-Barman et al.*, 2002; *Rutgers van der Loeff and Berger*, 1993]. The linearity of the increase in concentration with water depth is disturbed by the formation of NADW, which transports low concentrated surface waters to the deep. Furthermore, scavenged ^{231}Pa desorbs again from particles in the deep and can be exported with the southward flow path of NADW more readily than the more particle-reactive Th. On the way to the south, ^{230}Th regains linearity faster than ^{231}Pa because of its shorter steady state residence time in the water column. Therefore, even though there is a significant shallow (<2500 m) southward flow in the North Atlantic today [*Gherardi et al.*, 2010; *Schott et al.*, 2004; *Smethie and Fine*, 2001], it is not strong enough to produce a significant ^{231}Pa export and, as a consequence, sediments deposited above that depth do not exhibit a ^{231}Pa deficit relative to the overlying production [*Francois*, 2007; *Gherardi et al.*, 2010; *Luo et al.*, 2010]. On the other hand, the same overturning rate at greater depth produces a measurable deficit in deep sediments because of the longer residence time of ^{231}Pa in deep water [see also *Gherardi et al.*, 2010, Figure 1].

4.2. Model Versus Experimental Data

4.2.1. Model Description

[19] These complex interactions between genesis and reversible scavenging of ^{231}Pa and ^{230}Th and circulation strength in different water depths and latitudes respectively can be approximated using a simple 2D model [*Luo et al.*, 2010]. This model is based on a two-dimensional parameter set for ^{231}Pa and ^{230}Th adsorption and desorption derived from water column data and a modern depth distribution of lateral transport. The model results indicate that the relationship between Pa/Th at any given depth and the overturning circulation is very complex, as also noted by [*Siddall et al.*, 2005, 2007]. It reproduces many of the features observed in the distribution of dissolved and sedimentary Pa/Th and provides a tool to assess the relative importance of circulation and particle scavenging in controlling the distribution pattern of Pa/Th in the Atlantic. The most robust signals generated by the model are the vertical and horizontal sediment Pa/Th gradients, which change systematically with the rate and geometry of the AMOC [*Luo et al.*, 2010]. However, the model is proposed to simply reflect an averaged

longitudinal two-dimensional Pa/Th pattern, thus not capable of displaying west-east differences in circulation strength. Furthermore, the width of the Atlantic basin in the western equatorial region is the shortest, while a constant width for the entire Atlantic is assumed in the original model. Thus, the model underestimates the flow speed for the area of our examination. Hence, we modified the assumed circulation strength for NADW in the model and tested its general impact on the Pa/Th distribution in order to better mirror the specific situation of the western equatorial Atlantic. We note that although model circulation strengths higher than 20.5 Sv yield a better fit to the data, it does not imply higher circulation rates in reality. This rather results from the limitations of the 2D model to a 3D ocean (e.g., the reduced Atlantic basin width in the equatorial region). Below 1/3 of the assumed NADW strength of 20.5 Sv (Figure 4a) [*Macdonald*, 1998; *Talley et al.*, 2003], the Pa/Th–to-water depth connection collapses (for more details, see Figure S1). These sensitivity tests document the main impact on the depth distribution of Pa/Th, which is given by the assumed circulation strength in the depth range from approx. 1000 m to 4000 m.

4.2.2. Model Data Comparison

[20] The direct comparison of the model output at the equatorial section of the Atlantic Ocean to the observed Pa/Th profiles from this study shows generally a good agreement (Figure 4b) reflecting the depth dependence of Pa/Th. Sedimentary Pa/Th ratios are slightly lower than the model outputs, especially above 2500 m depth and below 4000 m where diverging results can also be observed. One potential bias of the model might be given by the flow path of NADW, which is not exclusive meridionally directed from North to South, as assumed by the 2D model. Thus, latitudes given by the model may slightly differ from the latitudes of the sediment core locations (see Figure S2).

[21] Further offsets between model and data are most likely caused by the variability and uncertainties of parameters used to constrain the model. Sinking rates as well as adsorption and desorption rate constants for ^{230}Th and ^{231}Pa have been chosen to be broadly consistent with field observation. Taking that into account, the similarity in the shape of the profiles is a positive result. Around the equator, the deeper waters may be influenced by the AABW [*Lynch-Stieglitz et al.*, 2007]. AABW is implemented in the 2D box model by *Luo et al.* [2010], but the discrepancy may point to an expansion of this water mass not fitted in a realistic way in the model.

[22] Nonetheless, within a reasonable range of model parameters, the very good agreement of theoretical and experimental data leads us to conclude that the 2D-box model by *Luo et al.* [2010] is capable of reflecting the Pa/Th system of the Atlantic Ocean in good agreement with measurement results. From this we conclude that the strong dependence of Pa/Th to water depth is caused by the AMOC, as predicted by the model and as actually observed.

[23] Thus, we propose that an inverse approach of tuning the model's depth distribution of lateral water transport based on Pa/Th data from time periods older than the Holocene may provide a promising way of reconstructing past AMOC.

5. Conclusion

[24] Here we compare depth-dependent sedimentary Pa/Th from one distinct oceanographic setting to predictions of a simple box model, which examined the behaviour of Pa/Th under recent circulation strength and particle flux conditions in the Atlantic Ocean.

[25] Our results fully support the Atlantic Pa/Th distribution described by *Luo et al.* [2010], displaying high values in shallow water (due to the longer residence time of ^{231}Pa compared to ^{230}Th) and low values in the deep (due to the export of ^{231}Pa with southward flowing NADW).

[26] Due to the very good agreement of experimental data and model results - and according to the sensitivity test made by *Luo et al.* [2010] - we conclude that ocean circulation is a main driver of the Pa/Th proxy. Therefore, its application for reconstruction of past AMOC seems reasonable and very promising, as long as changes in particle regimes are considered, and carefully reconstructed.

[27] **Acknowledgments.** The authors want to thank Roger Francois for constructive discussion; Siv Hjorth Dundas from Bergen Geoanalytical facility for supporting the ICP-MS measurements; Evelyn Böhm, Emanuel Christner, and Quentas Supiramaniam (Heidelberg Academy of Sciences) for supporting the chemical analyses; Jürgen Pätzold and Stefan Mulitza (MARUM Bremen) for providing sample material; and Marcus Gutjahr (University of Bristol) for MC-ICP-MS measurements. We thank Mathieu Daeron, Alexander Thomas, and two anonymous reviewers for improvement of the manuscript. This project was funded by the European Cooperation in Science and Technology "COST" (STSM action ES0801) and the German Science Foundation (DFG grant LI1815/2-1). This study used samples and data provided by the Bremen GeoB Core Repository. We also would like to acknowledge the crew of the research vessel Marion-Dufresne and the French Paul Emile Victor Institute (IPEV) for collecting the MD-cores presented here during the October 2009 scientific cruise led by C. Waelbroeck and T. Dokken within the framework of the ESF—EUROMARC project 'RETRO'.

[28] The Editor thanks Alex Thomas and Martin Frank for their assistance in evaluating this paper.

References

Anderson, R., M. Bacon, and P. Brewer (1983), Removal of ^{230}Th and ^{231}Pa from the open ocean, *Earth Planet. Sci. Lett.*, *62*, 7–23, doi:10.1016/0012-821X(83)90067-5.

Anderson, R., Y. Lao, and M. Fleisher (2009), Sedimentary Pa-231/Th-230 ratios are not a proxy for Atlantic meridional overturning circulation, *Geochim. Cosmochim. Acta*, *73*(13), A40.

Bacon, M., and R. Anderson (1982), Distribution of thorium isotopes between dissolved and particulate forms in the deep sea, *J. Geophys. Res.*, *87*, 2045–2056, doi:10.1029/JC087iC03p02045.

Bradtmiller, L., R. Anderson, M. Fleisher, and L. Burckle (2007), Opal burial in the equatorial Atlantic Ocean over the last 30 kyr: Implications for glacial-interglacial changes in the ocean silicon cycle, *Paleoceanography*, *22*, PA4216, doi:10.1029/2007PA001443.

Coppola, L., M. Roy-Barman, S. Mulsow, P. Povinec, and C. Jeandel (2006), Thorium isotopes as tracers of particles dynamics and deep water circulation in the Indian sector of the Southern Ocean (ANTARES IV), *Mar. Chem.*, *100*, 299–313, doi:10.1016/j.marchem.2005.10.019.

Dengler, M., F. Schott, C. Eden, P. Brandt, J. Fischer, and R. Zantopp (2004), Break-up of the Atlantic deep western boundary current into eddies at 8° S, *Nature*, *432*, 1018–1020, doi:10.1038/nature03134.

Francois, R. (2007), Paleoflux and paleocirculation from sediment ^{230}Th and $^{231}Pa/^{230}Th$, in *Proxies in Late Cenozoic Paleoceanography*, edited by C. Hillaire-Marcel and A. de Vernal, pp. 681–716, Elsevier, Amsterdam, doi:10.1016/S1572-5480(07)01021-4.

Gherardi, J., L. Labeyrie, S. Nave, R. Francois, J. McManus, and E. Cortijo (2009), Glacial-interglacial circulation changes inferred from $^{231}Pa/^{230}Th$ sedimentary record in the North Atlantic region, *Paleoceanography*, *24*, PA2204, doi:10.1029/2008PA001696.

Gherardi, J., Y. Luo, R. Francois, J. McManus, S. Allen, and L. Labeyrie (2010), Reply to comment by S. Peacock on "Glacial-interglacial circulation changes inferred from $^{231}Pa/^{230}Th$ sedimentary record in the North Atlantic region," *Paleoceanography*, *25*, PA2207, doi:10.1029/2009PA001867.

Hall, I., S. Moran, R. Zahn, P. Knutz, C. Shen, and R. Edwards (2006), Accelerated drawdown of meridional overturning in the late-glacial Atlantic triggered by transient pre-H event freshwater perturbation, *Geophys. Res. Lett.*, *33*, L16616, doi:10.1029/2006GL026239.

Keigwin, L., and E. Boyle (2000), Detecting Holocene changes in thermohaline circulation, *Proc. Natl. Acad. Sci. U. S. A.*, *97*(4), 1343–1346, doi:10.1073/pnas.97.4.1343.

Keigwin, D., and E. Boyle (2008), Did North Atlantic overturning halt 17,000 years ago?, *Paleoceanography*, *23*, PA1101, doi:10.1029/2007PA001500.

Lippold, J., J. Grützner, D. Winter, Y. Lahaye, A. Mangini, and M. Christl (2009), Does sedimentary $^{231}Pa/^{230}Th$ from the Bermuda Rise monitor past Atlantic meridional overturning circulation?, *Geophys. Res. Lett.*, *36*, L12601, doi:10.1029/2009GL038068.

Luo, Y., R. Francois, and S. Allen (2010), Sediment $^{231}Pa/^{230}Th$ as a recorder of the rate of the Atlantic meridional overturning circulation: Insights from a 2-D model, *Ocean Sci.*, *6*, 381–400, doi:10.5194/os-6-381-2010.

Lynch-Stieglitz, J., et al. (2007), Atlantic meridional overturning circulation during the Last Glacial Maximum, *Science*, *316*, 66–69, doi:10.1126/science.1137127.

Macdonald, A. (1998), The global ocean circulation: A hydrographic estimate and regional analysis, *Prog. Oceanogr.*, *41*, 281–382, doi:10.1016/S0079-6611(98)00020-2.

Marchal, O., R. Francois, T. Stocker, and F. Joos (2000), Ocean thermohaline circulation and sedimentary $^{231}Pa/^{230}Th$ ratio, *Paleoceanography*, *15*, 625–641, doi:10.1029/2000PA000496.

McManus, J., R. Francois, J. Gherardi, L. Keigwin, and S. Brown-Leger (2004), Collapse and rapid resumption of Atlantic meridional circulation linked to deglacial climate change, *Nature*, *428*, 834–837, doi:10.1038/nature02494.

Moran, S., C. Shen, S. Weinstein, L. Hettinger, J. Hoj, H. Edmonds, and R. Edwards (2001), Constraints on deep water age and particle flux in the equatorial and South Atlantic Ocean based on seawater ^{231}Pa and ^{230}Th data, *Geophys. Res. Lett.*, *28*, 3437–3440, doi:10.1029/2001GL013339.

Moran, S. B., C. C. Shen, H. N. Edmonds, S. E. Weinstein, J. N. Smith, and R. L. Edwards (2002), Dissolved and particulate ^{231}Pa and ^{230}Th in the Atlantic Ocean: constraints on intermediate/deep water age, boundary scavenging, and $^{231}Pa/^{230}Th$ fractionation, *Earth Planet. Sci. Lett.*, *203*, 999–1014, doi:10.1016/S0012-821X(02)00928-7.

Nozaki, Y., and T. Nakanishi (1985), ^{231}Pa and ^{230}Th profiles in the open ocean water column, *Deep Sea Res., Part A*, *32*, 1209–1220, doi:10.1016/0198-0149(85)90004-4.

Peacock, S. (2010), Comment on "Glacial-interglacial circulation changes inferred from $^{231}Pa/^{230}Th$ sedimentary record in the North Atlantic region" by J. M. Gherardi et al., *Paleoceanography*, *25*, PA2206, doi:10.1029/2009PA001835.

Roy-Barman, M. (2009), Modelling the effect of boundary scavenging on thorium and protactinium profiles in the ocean, *Biogeosciences*, *6*, 3091–3107, doi:10.5194/bg-6-3091-2009.

Roy-Barman, M., L. Coppola, and M. Souhaut (2002), Thorium isotopes in the Western Mediterranean Sea: An insight into the marine particle dynamics, *Earth Planet. Sci. Lett.*, *196*, 161–174, doi:10.1016/S0012-821X(01)00606-9.

Rutgers van der Loeff, M., and G. Berger (1993), Scavenging of ^{230}Th and ^{231}Pa near the Antarctic polar front in the South Atlantic, *Deep Sea Res., Part II*, *40*, 339–357.

Scholten, J., J. Fietzke, A. Mangini, D. Garbe-Schönberg, A. Eisenhauer, P. Stoffers, and R. Schneider (2008), Advection and scavenging: Effect on ^{230}Th and ^{230}Pa distribution off southwest-Africa, *Earth Planet. Sci. Lett.*, *271*, 159–169, doi:10.1016/j.epsl.2008.03.060.

Schott, F. A., M. Dengler, P. Brandt, K. Affler, J. Fischer, B. Bourlès, Y. Gouriou, R. L. Molinari, and M. Rhein (2003), The zonal currents and transports at 35°W in the tropical Atlantic, *Geophys. Res. Lett.*, *30*(7), 1349, doi:10.1029/2002GL016849.

Schott, F., R. Zantopp, L. Stramma, M. Dengler, J. Fischer, and M. Wibaux (2004), Circulation and deepwater export at the western exit of the subpolar North Atlantic, *J. Phys. Oceanogr.*, *34*, 817–843, doi:10.1175/1520-0485(2004)034<0817:CADEAT>2.0.CO;2.

Siddall, M., G. Henderson, N. Edwards, M. Frank, S. Müller, T. Stocker, and F. Joos (2005), $^{231}Pa/^{230}Th$ fractionation by ocean transport, biogenic particle flux and particle type, *Earth Planet. Sci. Lett.*, *237*, 135–155, doi:10.1016/j.epsl.2005.05.031.

Siddall, M., T. Stocker, G. Henderson, F. Joos, M. Frank, N. Edwards, S. Ritz, and S. Müller (2007), Modelling the relationship between $^{231}Pa/^{230}Th$ distribution in North Atlantic sediment and Atlantic meridional overturning circulation, *Paleoceanography*, *22*, PA2214, doi:10.1029/2006PA001358.

Smethie, W., and R. Fine (2001), Rates of North Atlantic Deep Water formation calculated from chlorofluorocarbon inventories, *Deep Sea Res., Part I*, *48*, 189–215, doi:10.1016/S0967-0637(00)00048-0.

Talley, L., J. Reid, and P. Robbins (2003), Data-based meridional overturning streamfunctions for the global ocean, *J. Clim.*, *16*, 3213–3226, doi:10.1175/1520-0442(2003)016<3213:DMOSFT>2.0.CO;2.

Tanhua, T., et al. (2009), CARINA Data Synthesis Project, http://cdiac.ornl.gov/oceans/CARINA/about_carina.html, Carbon Dioxide Inf. Anal. Cent, Oak Ridge, Tenn.

Thomas, A., G. Henderson, and L. Robinson (2006), Interpretation of the $^{231}Pa/^{230}Th$ paleocirculation proxy: New water-column measurements from the southwest Indian Ocean, *Earth Planet. Sci. Lett.*, *241*, 493–504, doi:10.1016/j.epsl.2005.11.031.

Yu, E., R. Francois, and M. Bacon (1996), Similar rates of modern and last-glacial ocean thermohaline circulation inferred from radiochemical data, *Nature*, *379*, 689–694, doi:10.1038/379689a0.

J.-M. Gherardi, LSCE, IPSL, CNRS/CEA/UVSQ, domaine du CNRS, F-91198 Gif-sur-Yvette CEDEX, France. (jeanne.gherardi@lsce.ipsl.fr)

J. Lippold, Heidelberg Academy of Sciences, Institute of Environmental Physics, University of Heidelberg, D-69120 Heidelberg, Germany. (joerg.lippold@iup.uni-heidelberg.de)

Y. Luo, Department of Earth and Ocean Sciences, University of British Columbia, 6270 University Blvd., Vancouver, BC V6T 1Z4, Canada.